

---

# Tangent Space Causal Inference: Leveraging Vector Fields for Causal Discovery in Dynamical Systems

---

**Kurt Butler\*** **Daniel Waxman\*** **Petar M. Djurić**

Department of Electrical and Computer Engineering

Stony Brook University

{kurt.butler, daniel.waxman, petar.djuric}@stonybrook.edu

## Abstract

Causal discovery with time series data remains a challenging yet increasingly important task across many scientific domains. Convergent cross mapping (CCM) and related methods have been proposed to study time series that are generated by dynamical systems, where traditional approaches like Granger causality are unreliable. However, CCM often yields inaccurate results depending upon the quality of the data. We propose the Tangent Space Causal Inference (TSCI) method for detecting causalities in dynamical systems. TSCI works by considering vector fields as explicit representations of the systems' dynamics and checks for the degree of synchronization between the learned vector fields. The TSCI approach is model-agnostic and can be used as a drop-in replacement for CCM and its generalizations. We first present a basic version of the TSCI algorithm, which is shown to be more effective than the basic CCM algorithm with very little additional computation. We additionally present augmented versions of TSCI that leverage the expressive power of latent variable models and deep learning. We validate our theory on standard systems, and we demonstrate improved causal inference performance across a number of benchmark tasks.

## 1 Introduction

The discovery of causal relationships is one of the most fundamental goals of scientific work. When causal relationships are known and understood, we can explain the behavior of a system and understand how our actions or interventions upon the system will affect its behavior [27]. This kind of reasoning is fundamental in many problem domains, such as medicine, environmental policy, and economics. However, it is not always possible to perform interventions and observe their effects. For example, medical practitioners might only have one chance to prescribe a medication to help a patient. As another example, an ecologist might find that performing a large experiment is forbiddingly expensive or otherwise infeasible. Due to these concerns, there remains a great interest in the problem of *observational* causal inference, where one infers causation without manipulating the system under study directly.

For time series data, the most prominent tool for observational causal inference is Granger causality [15]. Granger causality operates on the assumption that if one system (the cause) is driving changes in another system (the effect), then the cause should have unique information about what will happen to the effect. This is encoded in an assumption called *separability*, which posits that the information needed to predict the future behavior of the effect is not contained in the effect itself. However, the separability condition runs counter to the behavior of coupled dynamical systems: if long histories of the effect can forecast the cause, then an autoregressive model with the appropriate lag may forecast the effect from itself. This effect is explored in the supplementary materials of [12, 41], and we give

---

\*Equal contribution.

an example in Appendix B. Since systems with (approximately) dynamical behavior are ubiquitous in many application domains, alternative methods have become of interest.

To address the failures of Granger causality in coupled dynamical systems Sugihara et al. [41] proposed the convergent cross mapping (CCM) method, which directly takes advantage of the topological properties of dynamical systems. CCM can be seen as an adaption of earlier work that studied the synchronization of dynamical systems [2, 29, 35] into an algorithmic procedure for detecting causalities between time series. Using Takens’ theorem, a well-known result in dynamical systems theory [42], CCM attempts to detect causality by reconstructing the state space of a given time series, and then learning a time-invariant function that maps between reconstructed state spaces, called a cross map. The key assumption is that the cross map only exists if the original systems were dynamically coupled. In this sense, the “causality” of CCM deviates from the popular Pearlian framework [27], and is better interpreted as identifying which variables “drive” or “force” a dynamical system based on observational data.<sup>2</sup> Building upon this framework, several extensions of CCM have been proposed to address various technicalities and caveats of the approach and to generalize the method to new domains. However, the CCM test statistic is difficult to interpret and does not admit a simple decision rule. CCM also does not explicitly learn a cross map function.

To improve upon CCM, we propose Tangent Space Causal Inference (TSCI). TSCI detects causation between dynamical systems by explicitly checking if the dynamics of one system map on to the other. The proposed method can be seen as a drop-in replacement for the CCM test, providing an interpretable and principled alternative while remaining compatible with many of the extensions of CCM. Furthermore, the proposed method is model agnostic, meaning that it can be adapted to any method used to learn the cross map function, including multilayer perception (MLP) networks, splines, or Gaussian process regression. The only major assumption of TSCI is that the time series under study were generated by continuous time dynamical systems (i.e, by systems of differential equations), which is a standard assumption in a number of physical systems [36]. As a result, TSCI is applicable to many of the same problems as CCM.

## 1.1 Related Work

**Causal representation learning.** The primary function of Takens’ theorem in the CCM method is to yield a representation of a system’s latent state so that it may be used for cross mapping. As a result, numerous generalizations of Takens’ theorem emerged in the following decades [32, 33, 40]. Causal representation learning aims to learn hidden variables from high dimensional observations [1], and a principle task is to decipher the causal relationships between many, possibly redundant, observations of a system [30]. In such cases, methods of dimensionality reduction can be applied to extract causal variables from the raw observations [31]. This is particularly important in the processing of large, spatio-temporal data sets [36, 43]. Some authors have proposed that CCM can be improved by aggregating data from multiple sources into the reconstruction of the latent states [7, 45], which requires an awareness of how the observation data relate to the causal variables of interest.

**Causal discovery with cross maps.** CCM has popularized the use of cross maps as a tool for causal inference, and many variations and improvements of the basic CCM methodology have been proposed. Some of these works aim to improve the reconstruction of latent states in these models by using a Bayesian approach to latent state inference [13], where the approach is adapted for spatial/geographic data [14] or modified for sporadically sampled time series [12]. Additionally, several improvements have suggested changing the way that a cross map is detected: some authors have recommended varying the library length [25] or time delaying the cross mapping [44] to yield refined information. The  $k$ -nearest neighbor regression, which is used in the original CCM algorithm, can be swapped out for a radial basis function network [23], or for a Gaussian process regression model [13]. Other approaches have not directly learned the cross map at all; instead they have examined other aspects of the reconstructions such as their dimensionality [3] or used pairwise distance rankings as a signature of the mapping [5].

---

<sup>2</sup>Although not typically interpreted as such, cross maps have been suggested to be interpretable in a Pearlian causal framework via the  $do$  operator [12].

## 2 Proposed Method

We begin by considering the inference of a causal relationship between two time series,  $x(t)$  and  $y(t)$ . Our starting assumption is that both time series were generated by latent dynamical systems with states  $\mathbf{z}_x(t)$  and  $\mathbf{z}_y(t)$ , respectively, whose behavior is governed by a set of ordinary differential equations (ODEs). For motivation, we consider a particular case with a unidirectional coupling between the latent states:

$$x(t) = h_x(\mathbf{z}_x(t)), \quad (1)$$

$$y(t) = h_y(\mathbf{z}_y(t)), \quad (2)$$

$$\frac{d\mathbf{z}_x}{dt} = \mathbf{f}_x(\mathbf{z}_x), \quad (3)$$

$$\frac{d\mathbf{z}_y}{dt} = \mathbf{f}_y(\mathbf{z}_x, \mathbf{z}_y), \quad (4)$$

where the observation functions  $h_x, h_y$  and the time derivative functions  $\mathbf{f}_x, \mathbf{f}_y$  are assumed to be differentiable. A causal relationship between  $x$  and  $y$  is evidenced by the appearance of  $\mathbf{z}_x$  in the equation for  $d\mathbf{z}_y/dt$ . The state vectors  $\mathbf{z}_x$  and  $\mathbf{z}_y$  could possibly have redundant information, but by writing the system in this form, we obtain an asymmetry between  $x(t)$  and  $y(t)$  which will inform our inference of causation. In our notation, if  $\mathbf{z}_x$  appears in the equation for  $d\mathbf{z}_y/dt$ , we will write  $x \rightarrow y$ .

We now explain how the CCM method approaches this problem and how the TSCI method builds upon the CCM framework.

### 2.1 Convergent Cross Mapping

CCM is a technique for inferring causation between time series generated by dynamical systems [41], as seen in Eqs. (1) to (4). The basic motivation for CCM is that given an observed time series  $x(t)$ , one can construct a vector  $\tilde{\mathbf{x}}$  which acts as a proxy for the latent states  $\mathbf{z}_x$  that generated it. Given two constructions,  $\tilde{\mathbf{x}}$  and  $\tilde{\mathbf{y}}$ , we may detect if there is a mapping between them, which provides evidence of a causal relationship. From Eq. (4), since  $\mathbf{z}_x$  influences  $\mathbf{z}_y$  unidirectionally, the effect  $y(t)$  contains more information than the cause time series  $x(t)$ , and as a result  $\tilde{\mathbf{y}}$  generally contains enough information to reconstruct  $\tilde{\mathbf{x}}$ . With this in mind, we can frame CCM as a two-step procedure [13]. In Step 1, we construct representations  $\tilde{\mathbf{x}}$  and  $\tilde{\mathbf{y}}$  that are proxies for  $\mathbf{z}_x$  and  $\mathbf{z}_y$ , respectively. In Step 2, we detect a mapping between reconstructions; if there is a mapping  $\tilde{\mathbf{y}} \mapsto \tilde{\mathbf{x}}$ , then the reverse causality holds,  $x \rightarrow y$ .

To reconstruct the latent state space, as in Step 1, multiple approaches could be employed. However, in the basic CCM methodology, one uses the so-called *delay embedding* of  $x(t)$ ,

$$\tilde{\mathbf{x}}(t) = \begin{bmatrix} x(t) \\ x(t - \tau) \\ \vdots \\ x(t - (Q - 1)\tau) \end{bmatrix}, \quad (5)$$

where  $\tau$  and  $Q$  are parameters called the embedding lag and embedding dimension, respectively. The justification that  $\tilde{\mathbf{x}}$  is a good proxy for  $\mathbf{z}_x$  is given by Takens' theorem [42], which states that  $\tilde{\mathbf{x}}$  and  $\mathbf{z}_x$  are equivalent up to a nonlinear change of coordinates.

**Theorem 2.1 (Takens' theorem [33])** *Let  $M$  be a compact manifold of dimension  $d$ . Let  $\mathbf{z} \in M$  evolve according to  $d\mathbf{z}/dt = \mathbf{f}(\mathbf{z})$ , let  $\phi_\tau$  be the mapping that takes  $\mathbf{z}_t$  to  $\mathbf{z}_{t+\tau}$ , and let  $x(t) = h(\mathbf{z}(t))$ . If  $Q \geq 2d + 1$ , then for almost-every<sup>3</sup> triplet  $(\mathbf{f}, h, \tau)$ , the map  $\Phi_{\mathbf{f}, h, \tau}$*

$$\Phi_{\mathbf{f}, h, \tau}(\mathbf{z}) = \begin{bmatrix} h(\mathbf{z}) \\ h(\phi_{-\tau}(\mathbf{z})) \\ \vdots \\ h(\phi_{-(Q-1)\tau}(\mathbf{z})) \end{bmatrix} \quad (6)$$

<sup>3</sup>Several versions of Takens' theorem exist, and they make useful, but mathematically distinct, statements about how common such embeddings are. The version presented here says that functions that do *not* produce embeddings live on a measure zero set, in the sense of prevalence [33, p. 584].

is an embedding of  $M$  into  $\mathbb{R}^Q$ .

Since  $\Phi_{f,h,\tau}(\mathbf{z}_x(t)) = \tilde{\mathbf{x}}(t)$ , Takens' theorem tells us that if  $\mathbf{z}_x$  lives on a manifold  $M$ , then the points  $\tilde{\mathbf{x}}$  lie on a manifold  $\mathcal{M}_x$ , which is called the *shadow manifold* of  $x$  [41]. Despite the number of assumptions in the statement of Takens' theorem, many generalizations of the statement exist, allowing us to justify the use of delay embedding to systems with strange attractors [33] and systems with noise [40]. If a system satisfies the conditions for Takens' theorem, in the sense that  $\mathcal{M}_x$  is a valid embedding of  $M$ , then we say that the system is *generic*.

Since only  $\mathbf{z}_x$  influences  $x(t)$ , Takens' theorem implies that  $\tilde{\mathbf{x}}$  is equivalent (up to nonlinear coordinate change) to  $\mathbf{z}_x$ . However, due to the appearance of  $\mathbf{z}_x$  in (4), both  $\mathbf{z}_x$  and  $\mathbf{z}_y$  are responsible for generating  $y(t)$ . As a result, Takens' theorem suggests that  $\tilde{\mathbf{y}}$  is equivalent to  $(\mathbf{z}_x, \mathbf{z}_y)$  as a concatenated vector [39]. Since  $(\mathbf{z}_x, \mathbf{z}_y)$  clearly can be mapped onto  $\mathbf{z}_x$ , the equivalence between the delay embeddings and the latent states suggests that there is a mapping  $\tilde{\mathbf{y}} \mapsto \tilde{\mathbf{x}}$ , called a *cross map*. Thus, cross maps encode the idea that the effect time series contains information about its cause. This is encoded in the following corollary to Takens' theorem.

**Corollary 2.1.1** *Suppose that  $x \rightarrow y$  for a generic system. Then there exists a function  $F$  such that  $\tilde{\mathbf{x}}(t) = F(\tilde{\mathbf{y}}(t))$  for all  $t$ .*

The proof of the corollary is provided in the Appendix.

Step 2 of CCM is then to detect if  $x \rightarrow y$  by checking if a cross map  $\tilde{\mathbf{y}} \mapsto \tilde{\mathbf{x}}$  exists. To this end, Sugihara et. al. [41] propose to check the predictability of the time series  $x(t)$  given  $\tilde{\mathbf{y}}(t)$ . They use a form of  $k$ -nearest neighbors regression to produce an estimate  $\hat{x}(t)$  of  $x(t)$  given  $\tilde{\mathbf{y}}(t)$ , and then they define a test statistic

$$r_{X \rightarrow Y}^{\text{CCM}} = \text{corr}(\hat{x}(t), x(t)), \quad (7)$$

where  $\text{corr}$  is the Pearson correlation coefficient. To test the reverse causal direction,  $x \leftarrow y$ , one simply performs Step 2 again with the roles of  $x$  and  $y$  reversed.

## 2.2 Tangent Space Causal Inference

Takens' theorem and cross maps as a tool for causal inference are rooted in a solid mathematical foundation, but the CCM test does not exploit all of the properties of shadow manifolds. Namely, it does not exploit the fact that the shadow manifolds are copies of the latent manifolds. In practice, there are cases in which CCM learns a cross map that appears to be reasonably predictive, but results in a false positive. Thus, a more robust algorithm would exploit more subtle properties of the hypothesized cross map. We propose TSCI as alternative to Step 2 in the CCM algorithm.

TSCI operates by checking if the ODE on one manifold,  $\mathcal{M}_x$ , can be mapped to an ODE on another manifold  $\mathcal{M}_y$ . To understand how this works, we need to reframe our discussion of ODEs in terms of vector fields. Recall that given an ODE of the form,

$$\frac{d\tilde{\mathbf{x}}}{dt} = \mathbf{u}(\tilde{\mathbf{x}}), \quad (8)$$

we may interpret  $\mathbf{u}$  to be a velocity vector field on the manifold. When evaluated,  $\mathbf{u}(\tilde{\mathbf{x}})$  is a tangent vector of the manifold  $\mathcal{M}_x$ , existing in the tangent space  $T_{\tilde{\mathbf{x}}}\mathcal{M}_x$ <sup>4</sup>. From calculus, we know that tangent vectors in  $T_{\tilde{\mathbf{x}}}\mathcal{M}_x$  can be mapped to tangent vectors in  $T_{F(\tilde{\mathbf{x}})}\mathcal{M}_y$  by the Jacobian matrix  $\mathbf{J}_F(\tilde{\mathbf{x}})$  at the point  $\tilde{\mathbf{x}}$ . By checking if the tangent vectors can be mapped in such a way, TSCI provides an alternative to the CCM causality test. A visual motivation for the TSCI methods is depicted in Fig. 1.

Before we can map vector fields from one manifold to another, we need to check that meaningful vector fields exist on the shadow manifolds. As usual, this is also a corollary of Takens' theorem.

**Corollary 2.1.2** *There exists a vector field  $\mathbf{u}$  on  $\mathcal{M}_x$  such that the embedding  $\Phi_{f,h,\tau}$  in Takens' theorem is a time-invariant mapping. If we define  $\gamma(0) = \Phi_{f,h,\tau}(\mathbf{z}_x(0))$ , and if we let  $\gamma(t)$  to be the flow of a point  $\gamma(0)$  under the vector field  $\mathbf{u}$ , then  $\Phi_{f,h,\tau}(\mathbf{z}_x(t)) = \gamma(t)$ , for all times  $t$ .*

<sup>4</sup>See Appendix A for definitions of differential geometric quantities such as the tangent space.

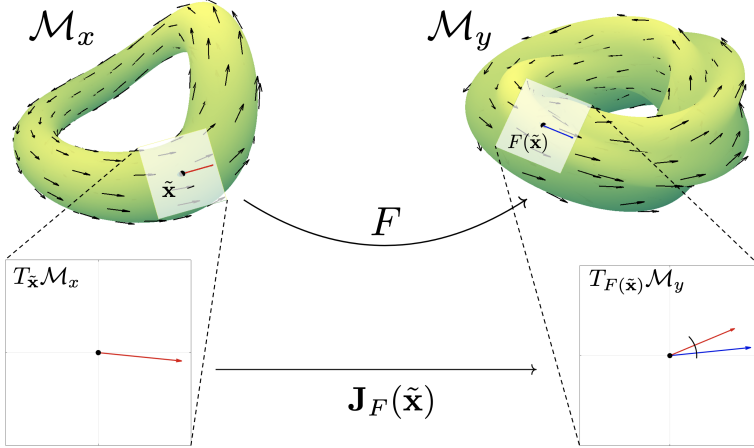


Figure 1: Visual motivation for the TSCI method. Observed time series are related to latent states evolving on some manifolds. Given observed time series  $x(t)$  and  $y(t)$ , we reconstruct latent states  $\tilde{x}(t)$  and  $\tilde{y}(t)$  that reside in manifolds  $\mathcal{M}_x$  and  $\mathcal{M}_y$ , respectively. If  $x$  and  $y$  are causally coupled, there should exist a function  $F$  that maps between these manifolds. Using the Jacobian matrix  $\mathbf{J}_F$ , we can map the velocity vector field on  $\mathcal{M}_x$  to a vector field on  $\mathcal{M}_y$ , and use the angle between velocity vectors as a measure of their similarity.

The proof of the corollary is provided in the Appendix.

The corollary guarantees that we can learn ODEs that describe the dynamics of  $\tilde{x}$  and  $\tilde{y}$ , once we have obtained valid reconstructions of the latent states. Let  $\mathbf{u}$  and  $\mathbf{v}$  be vector fields such that

$$\frac{d\tilde{x}}{dt} = \mathbf{u}(\tilde{x}), \quad (9)$$

$$\frac{d\tilde{y}}{dt} = \mathbf{v}(\tilde{y}). \quad (10)$$

Because the cross map  $F$  is a mapping between the two shadow manifolds, the Jacobian matrix of the cross map relates the vectors  $\mathbf{u}$  and  $\mathbf{v}$ . We state this formally in the following Lemma.

**Lemma 2.1.1** *Let  $\mathcal{M}_x$  and  $\mathcal{M}_y$  be manifolds with respective vector fields  $\mathbf{u}$  and  $\mathbf{v}$  that define their dynamics. If there exists a cross map  $F : \mathcal{M}_x \rightarrow \mathcal{M}_y$ , then for every point  $\tilde{x} \in \mathcal{M}_x$ , we have that  $\mathbf{v}(F(\tilde{x})) = \mathbf{J}_F(\tilde{x})\mathbf{u}(\tilde{x})$ , where  $\mathbf{J}_F(\tilde{x})$  is the Jacobian matrix of  $F$  at  $\tilde{x}$ .*

The proof of the lemma is in the Appendix.

While the cross map  $F : \mathcal{M}_x \rightarrow \mathcal{M}_y$  is a mapping between points on the manifolds, the Jacobian matrix  $\mathbf{J}_F(\tilde{x})$  induces a mapping between the tangent spaces at  $\tilde{x}$  and  $\tilde{y}$ . We show this visually in Fig. 1. Since the velocity of  $\tilde{x}$  can be represented by a tangent vector  $\mathbf{u}(\tilde{x})$ , the Jacobian matrix  $\mathbf{J}_F$  allows us to map these vectors to tangent vectors in  $\mathcal{M}_y$ . If there is a cross map, then the vector field  $\mathbf{v}$  and the push forward vector field  $\mathbf{J}_F\mathbf{u}$  should match exactly. On the other hand, there should be no correlation in the absence of a causal relationship, assuming quality reconstructions and plentiful data. The degree of alignment between  $\mathbf{v}$  and  $\mathbf{J}_F\mathbf{u}$  can be used as a test statistic for the presence of a causal link. We therefore propose the TSCI test statistic,

$$r_{X \rightarrow Y}^{\text{TSCI}} = \text{corr}(\mathbf{u}, \mathbf{J}_F\mathbf{v}). \quad (11)$$

Because the tangent vectors are centered in their respective tangent planes, we can geometrically interpret the TSCI test statistic as the expected cosine similarity between the vector field  $\mathbf{u}$  and the push forward vector field  $\mathbf{J}_F\mathbf{v}$ ,

$$r_{X \rightarrow Y}^{\text{TSCI}} = \mathbb{E}_{\tilde{y} \sim \mathcal{M}_y} \left( \frac{\mathbf{u}(F(\tilde{y}))^\top \mathbf{J}_F(\tilde{y})\mathbf{v}(\tilde{y})}{\|\mathbf{u}(F(\tilde{y}))\| \|\mathbf{J}_F(\tilde{y})\mathbf{v}(\tilde{y})\|} \right). \quad (12)$$

In practice, the estimation quality of the cross map also depends on the location in the reconstruction space, and so the cosine similarity takes on a distribution of values (Fig. 2), and weak-to-moderate correlation may be empirically observed as an artifact of limited data.

---

**Algorithm 1** TANGENT SPACE CAUSAL INFERENCE

---

**Input:** Embedding/vector field matrices  $\mathbf{X}, \mathbf{U} \in \mathbb{R}^{T \times Q_x}$  and  $\mathbf{Y}, \mathbf{V} \in \mathbb{R}^{T \times Q_y}$

**Output:** Score  $r_{X \rightarrow Y}$

- 1: Learn a differentiable function  $F$  such that  $\mathbf{X}_t = F(\mathbf{Y}_t)$  for all  $t$
- 2: **for**  $t = 0, 2, \dots, T - 1$  **do**
- 3:     Compute the Jacobian matrix  $\mathbf{J}_F(\mathbf{Y}_t) \in \mathbb{R}^{Q_x \times Q_y}$  of the function  $F$  at location  $\mathbf{Y}_t$
- 4:     Push forward the tangent vector by computing  $\hat{\mathbf{U}}_t = \mathbf{V}_t \mathbf{J}_F^\top(\mathbf{Y}_t)$
- 5: **end for**
- 6: Define  $r_{X \rightarrow Y} = \text{corr}(\hat{\mathbf{U}}, \mathbf{U})$

---

**Algorithm 2** TANGENT SPACE CAUSAL INFERENCE WITH K-NEAREST NEIGHBORS

---

**Input:** Embedding/vector field matrices  $\mathbf{X}, \mathbf{U} \in \mathbb{R}^{T \times Q_x}$  and  $\mathbf{Y}, \mathbf{V} \in \mathbb{R}^{T \times Q_y}$ , regression parameter  $K > \max(Q_x, Q_y)$

**Output:** Score  $r_{X \rightarrow Y}$

- 1: **for**  $t = 0, 2, \dots, T - 1$  **do**
- 2:     Find the indices  $\tau_1, \dots, \tau_K$  of the  $K$ -nearest neighbors of  $\mathbf{Y}_t$
- 3:     Compute the local displacements in  $x$ -space:  $\Delta \mathbf{X}_k = \mathbf{X}_{\tau_k} - \mathbf{X}_t$
- 4:     Compute the local displacements in  $y$ -space:  $\Delta \mathbf{Y}_k = \mathbf{Y}_{\tau_k} - \mathbf{Y}_t$
- 5:     Compute the least-squares solution to  $\Delta \mathbf{Y}_k \mathbf{J} = \Delta \mathbf{X}_k$
- 6:     Compute  $\hat{\mathbf{U}}_t = \mathbf{V}_t \mathbf{J}$
- 7: **end for**
- 8: Define  $r_{X \rightarrow Y} = \text{corr}(\hat{\mathbf{U}}, \mathbf{U})$

---

Based on these analyses, we propose the TSCI method in Algorithm 1, which learns a cross-map  $F$  and returns the alignment of the vector fields  $\mathbf{u}$  and  $\mathbf{J}_F \mathbf{v}$ . CCM is sensitive to the quality of the reconstruction of the latent states because an improperly constructed shadow manifold can sabotage the method, both theoretically and empirically [6]; TSCI similarly requires that the shadow manifold be properly embedded. Because of this, we assume that the embedding vectors  $\tilde{\mathbf{x}}$  and  $\tilde{\mathbf{y}}$  and the estimates of their vector fields  $\mathbf{u}(\tilde{\mathbf{x}})$  and  $\mathbf{v}(\tilde{\mathbf{y}})$  at each point are supplied as inputs to the algorithm. A variety of methods could be used to estimate the vector fields, but the simplest approach is to use finite differences,

$$\mathbf{u}(\tilde{\mathbf{x}}) = \frac{d\tilde{\mathbf{x}}}{dt} = \begin{bmatrix} \frac{dx(t)}{dt} \\ \frac{dx(t-\tau)}{dt} \\ \vdots \\ \frac{dx(t-(Q-1)\tau)}{dt} \end{bmatrix} \approx \frac{1}{\Delta t} \begin{bmatrix} x(t+1) - x(t) \\ x(t+1-\tau) - x(t-\tau) \\ \vdots \\ x(t+1-(Q-1)\tau) - x(t-(Q-1)\tau) \end{bmatrix},$$

where  $\Delta t$  is the sampling rate of the data. Finite differences are known to be sensitive to noise, so in real scenarios a more careful approach to obtaining the time derivatives is necessary. For a practical implementation, we propose using the central finite-differences, which are second-order accurate [16], or the derivatives interpolated by a Savitsky-Golay filter for noisy data [34].

**On methods to learn the cross map function.** The TSCI algorithm is notably agnostic to the regression approach used for the cross map  $F$ , with reasonable approaches including multilayer perceptron networks (MLPs), splines, and Gaussian process regression (GPR). Depending on the approach, derivatives can then be estimated from the model, either using automatic differentiation or analytical derivatives. For GPR in particular, analytical derivatives are straightforward to compute [38].

Since regression can sometimes be a computationally complex procedure, in Algorithm 2 we also provide a version of TSCI that is based on the  $k$ -nearest regression, in analogy to CCM. For clean and dense data, this simple approach can yield accurate results, but it is generally unsuitable for noisy or sparse data. In the latter case, it is preferable to combine the TSCI approach with other methods of denoising time series, or learning of latent dynamical models of the observed time series. In particular, the learning of a latent ODE learning [12] can be combined with the TSCI test to yield accurate causal inference.

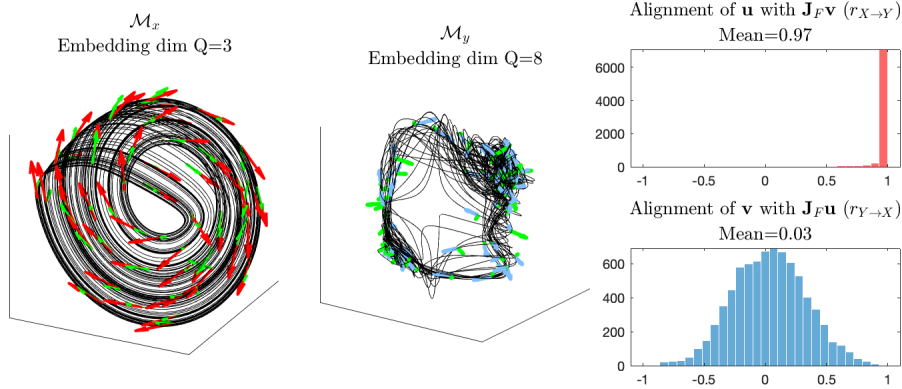


Figure 2: Shadow manifolds  $\mathcal{M}_x$  and  $\mathcal{M}_y$  from the unidirectionally coupled Rössler-Lorenz system Eq. (13) with  $C = 1$ , and the corresponding histograms of  $\hat{\mathbf{u}}^\top \mathbf{u}$  and  $\hat{\mathbf{v}}^\top \mathbf{v}$ . The test statistics,  $r_{X \rightarrow Y}$  and  $r_{X \leftarrow Y}$ , correspond to the means of these distributions.

**On the use of correlation coefficient.** In relation to CCM, it can be noted that both TSCI and CCM use a correlation coefficient as their test statistic. However, a critical difference between the two methods is how the usage of this statistic is justified. The correlation coefficient used in CCM analysis, called the cross-map skill [41], is used to measure the accuracy of predictions of the cross map. However, since the points being predicted in CCM live on a manifold, measuring correlation in the ambient (extrinsic) space is not well-motivated. Furthermore, estimates of this correlation can be biased by the distribution of observations along the manifold, and as a result, a high correlation can be achieved with a relatively low-accuracy prediction by guessing the general region in which the points lie.

In contrast, the correlation between tangent vectors (or vector fields) is a more geometrically motivated quantity: the correlation is a linear measure of similarity and the tangent vectors belong to a (centered) linear space. Additionally, the shadow manifolds are constructed to be submanifolds of Euclidean space, so correlations computed in extrinsic coordinates will match correlations computed using the intrinsic coordinates of the shadow manifold. By Lemma 2.1.1, the correlations will be identically 1 if a cross map exists.

One alternative to the cosine similarity is the mutual information (MI). Specialized to the current text, the MI  $I(\mathbf{u}; \mathbf{J}_F \mathbf{v})$  quantifies the reduction in the uncertainty of  $\mathbf{u}$  given the pushforward vector  $\mathbf{J}_F \mathbf{v}$  [9]. While the information-theoretic underpinning of the MI is attractive, we have two main reasons to prefer the cosine similarity: First, the MI between two (continuous) distributions can be difficult to interpret. For example, it is not obvious if  $I(\mathbf{u}; \mathbf{J}_F \mathbf{v}) = 0.5$  is a strong dependence or not, particularly in the case of continuous distributions. The cosine similarity, on the other hand, is upper bounded by 1, so  $\text{corr}(\hat{\mathbf{U}}, \mathbf{U}) = 0.95$  is easily interpreted as having near-perfect reconstruction. Second, accurate estimation of the MI from samples is a notoriously difficult task, particularly in high dimensions, and no single estimator works consistently well [10]. We provide some experiments with the MI, and show the differing performance of different estimators, in Appendix B.3.

### 3 Experiments

We validate the performance of TSCI on two datasets that are popular in the literature. The first arises from a coupled Rössler-Lorenz system, where the ground truth causality is known and the causal influence can be smoothly modulated. The second example was proposed in [12] and uses sporadic time series from coupled double pendulums, and illustrates the applicability of TSCI to extensions of CCM. Code implementing TSCI is available at <https://github.com/KurtButler/tangentspaces>. All comparisons to CCM use the `skccm` module in Python<sup>5</sup>. Experiments were run on a 6-Core Intel Core i5 and NVIDIA Titan RTX.

<sup>5</sup><https://github.com/nickc1/skccm>, MIT License

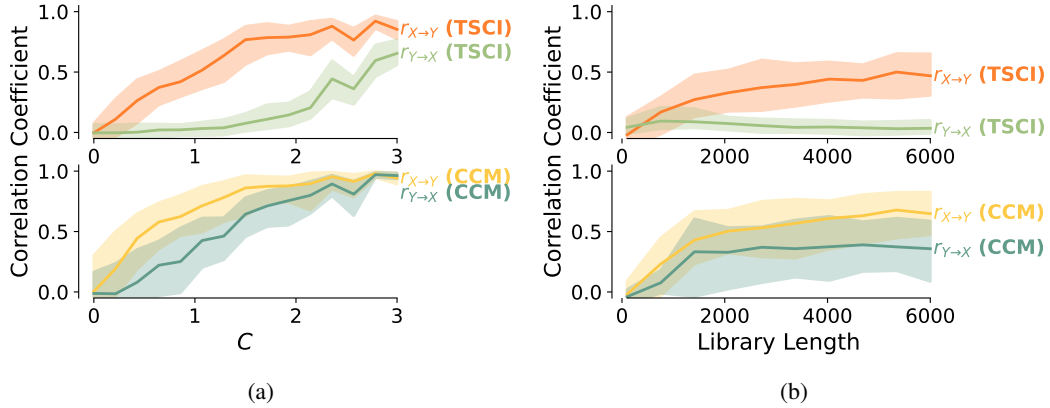


Figure 3: Comparison of TSCI with CCM for the Rössler-Lorenz system (true causation  $X \rightarrow Y$ ). The plotted lines show the median test statistic over 100 trials for both CCM and TSCI, and the shaded region indicates the 5th and 95th percentiles when (a)  $C$  is varied from 0 (no coupling) to 3 (approximate general synchrony), and (b)  $C$  is fixed to 1.0 and the library length is varied.

### 3.1 Unidirectionally-Coupled Rössler-Lorenz System

A common toy system used for studying coupled dynamic systems is a unidirectionally-coupled Rössler-Lorenz system [28], which we define in Eq. (13). In this system, the first three coordinates ( $z_1, z_2, z_3$ ) describe a Rössler system, and they are unidirectionally coupled with a Lorenz-type system ( $z_4, z_5, z_6$ ). The strength of the coupling is controlled by the parameter  $C$ . When  $C = 0$ , the two systems are disconnected, but for  $C > 0$  there is a causal influence from  $z_1, z_2, z_3$  to  $z_4, z_5, z_6$ .

$$\frac{dz}{dt} = \frac{d}{dt} \begin{bmatrix} z_1 \\ z_2 \\ z_3 \\ z_4 \\ z_5 \\ z_6 \end{bmatrix} = \begin{bmatrix} -6(z_{2,t} + z_{3,t}) \\ 6(z_{1,t}) + 0.2z_{2,t} \\ 6(0.2 + z_{3,t}(z_{1,t} - 5.7)) \\ 10(z_{5,t} - z_{4,t}) \\ 28z_{4,t} - z_{5,t} - z_{4,t}z_{6,t} + Cz_{2,t}^2 \\ z_{4,t}z_{5,t} - 8z_{6,t}/3 \end{bmatrix} \quad (13)$$

In Fig. 2, we visualize the TSCI method for  $x = z_2$  and  $y = z_4$ . First, we show the shadow manifolds  $\mathcal{M}_x$  and  $\mathcal{M}_y$  with a set of tangent vectors on each manifold. The delay embedding dimension parameters,  $Q_x$  and  $Q_y$ , were selected using the false-nearest neighbors algorithm with a tolerance of 0.005 [19]. Time lags for the embeddings,  $\tau_x$  and  $\tau_y$ , were selected by picking the minimal delay such that the autocorrelation function drops below a threshold [21]. Additionally, we show the histograms of  $\cos(\theta)$ , where  $\theta$  is the angle between the tangent vectors at each point. For  $X \rightarrow Y$  direction, which is the true causal direction, the distribution is concentrated near 1. For the  $Y \leftarrow X$  direction, the distribution of tangent vectors is centered on 0. The test statistics,  $r_{X \rightarrow Y}$  and  $r_{Y \rightarrow X}$ , correspond to the means of each distribution, and visibly correspond to the correct causality.

We show the effects of varying the coupling strength  $C$  in Fig. 3a, where TSCI clearly shows better separation across varying  $C$ . We see the effect of increasing the library length (i.e., the size of the training set in nearest neighbors) for  $C = 1.0$  in Fig. 3b. Here,  $r_{X \rightarrow Y}$  increases at similar rates for TSCI and CCM, suggesting similar data efficiency of the two methods.

### 3.2 Double Pendulum System

To illustrate the generality of TSCI within CCM-like frameworks, we applied the TSCI methodology to the latent CCM framework, where CCM is applied to a state-space reconstruction obtained via neural ODEs [12]. One reason to favor this approach is when the observed time series are irregularly (i.e., with a non-uniform sampling rate) or sporadically (i.e., any given observation only measures a subset of states) sampled. Notable for TSCI is the fact that ground-truth derivatives are available, as they are directly learned in the neural ODE reconstruction.

Table 1: Double Pendulum Experiments. Entries denote the mean  $\pm$  one standard deviation across 5 folds. Bolded directions indicate ground truth causality.

| Direction         | $r_{X_1 \rightarrow X_2}$ |                    |                    |
|-------------------|---------------------------|--------------------|--------------------|
|                   | Latent CCM                | Latent CCM (MLP)   | Latent TSCI (MLP)  |
| $X \rightarrow Y$ | $0.011 \pm 0.009$         | $0.015 \pm 0.009$  | $0.021 \pm 0.010$  |
| $X \rightarrow Z$ | $0.044 \pm 0.008$         | $0.055 \pm 0.011$  | $0.077 \pm 0.013$  |
| $Y \rightarrow X$ | $-0.003 \pm 0.008$        | $-0.005 \pm 0.009$ | $-0.010 \pm 0.004$ |
| $Y \rightarrow Z$ | $0.003 \pm 0.006$         | $-0.002 \pm 0.004$ | $-0.008 \pm 0.013$ |
| $Z \rightarrow X$ | $0.737 \pm 0.019$         | $0.747 \pm 0.015$  | $0.915 \pm 0.006$  |
| $Z \rightarrow Y$ | $0.475 \pm 0.043$         | $0.578 \pm 0.030$  | $0.612 \pm 0.053$  |

We replicate an experiment in the latent CCM paper where a network of unidirectionally coupled double pendulums are simulated, and observations sampled irregularly and sporadically. The authors' source code<sup>6</sup> was used to generate data and apply latent CCM. For more information on the data generation, see Appendix A of [12].

For TSCI, we learn a cross-map using an MLP between the reconstructed state spaces. To avoid tuning learning rates for every network, the parameter-free COCOB optimizer [26]<sup>7</sup> and networks were trained for 50 epochs. Results can be found in Table 1.

When compared to latent CCM, TSCI provided larger correlation coefficients for the true positive cases, with similarly small coefficients for the true negative cases. The use of MLPs for learning the cross map partially but not fully explains the difference in performance.

### 3.3 Additional Experiments

Several additional experiments appear in Appendix B. We briefly describe them here and provide some commentary on their results.

**Varying the embedding dimension.** In Appendix B.1, we artificially lower quality embeddings by varying the embedding dimension. We find that the performance of TSCI and CCM similarly degrade when using an embedding dimension that is very small, and that there is little harm to a larger embedding dimension. In either case, the hyperparameters from a false-nearest neighbors test perform well.

**Corrupting signals.** In Appendix B.2, we lower the embedding quality in two different ways: (1) by injecting additive noise to all observations, and (2) by adding a sine wave to observations. We observe that TSCI and CCM similarly degrade when the signal-to-noise ratio is altered. However, because of the larger separation in TSCI, the correct causal relation can be determined at much lower signal-to-noise ratios.

**Using mutual information.** In Appendix B.3, we experiment with using mutual information instead of cosine similarity. We find that conclusions made using MI are generally similar to those from cosine similarity, but with less interpretability and significant difficulties in estimation.

**Comparisons to other causal discovery methods.** As mentioned in the introduction, CCM (and hence TSCI) are specifically designed to address failures of Granger causality. In Appendix B.4, we empirically verify the limitations of Granger causality on our Rössler-Lorenz toy system. We additionally test several other causal discovery methods and show their limitations in our setting.

## 4 Advantages and Limitations of TSCI

**Scalability.** The TSCI approach, using the  $K$ -nearest neighbors algorithm, retains the scalability and lightweight implementation that CCM enjoys. The only additional computational complexity arises

<sup>6</sup><https://github.com/edebrouwer/latentCCM>, MIT License

<sup>7</sup><https://github.com/bremen79/parameterfree>, MIT License

from solving a local linear system of equations, and from the estimation of derivatives. Since the linear systems have a fixed size  $K$ , and since derivative estimation can be done using a linear filter, the additional cost is minimal. The general version of TSCI will scale depending on the choice of the regressor used to learn the cross map, and on other design decisions made to improve the efficacy of the method. However, this is not unlike the situation in which CCM is augmented with other customization options that potentially slow down the method.

**Model agnosticism.** Because a TSCI test can be formulated for any differentiable regression model used to learn the cross map, the approach is highly flexible and model agnostic. Additionally, because there are many potential ways in which reconstruction of latent states and learning of the velocity vector fields can be improved, the TSCI method can be incorporated into a wide variety of inference frameworks.

**Quality of reconstructed states.** In both CCM and TSCI, there are a few assumptions which warrant some justification before use, since their violation may yield to misapplication of cross map methods. The first issue is that while Takens' theorem implies that embeddings are plentiful, not all embeddings are equal in quality or useful. Shadow manifolds that are sparsely or incompletely sampled, time series with trends, or otherwise data which do not accurately capture the latent manifold can lead to dubious results using CCM [6]. While TSCI is less likely to produce a false positive in these cases, the assumption that a latent manifold is well-represented by a given embedding is nontrivial and critical to ensuring trustworthy performance of the method.

**General synchrony.** General synchrony is a problem that plagues all cross map-based methods [41]. The issue is that when the causal strength of the relationship  $x \rightarrow y$  is very strong, the influence of  $\mathbf{z}_x$  dominates the dynamics of  $\mathbf{z}_y$ , and  $\mathbf{z}_y$  cannot exhibit its own independent behavior. As a result,  $\mathcal{M}_y$  will look similar to  $\mathcal{M}_x$ , and the cross map will become an invertible function. As a result, a strong unidirectional relationship is detected as a bidirectional causal relationship. In Fig. 3, the Rössler-Lorenz system enters general synchrony near  $C = 3$  [6]. The TSCI method appears more resistant to the effects of general synchrony than CCM, but it is a topological fact that as  $C$  grows, synchrony becomes inevitable.

## 5 Conclusion

In this paper, we presented the TSCI method for detecting causation in dynamical systems. By considering how tangent vectors map from one manifold to another, we may achieve more robust detection of causal relationships in dynamical systems than with standard CCM. Key advantages of TSCI include that we may use it in many systems in which CCM would be applied, but the method is far less prone to false positives and spurious causation. We presented both a general form of the algorithm as well as a  $k$ -nearest neighbor version inspired by the original CCM algorithm. Because TSCI requires us to estimate latent states and their time derivatives, there is much room for the TSCI method to be further developed in future work.

## Acknowledgments and Disclosure of Funding

We would like to thank the anonymous reviewers for their suggestions which improved the content and presentation of this work. This work was supported by the National Science Foundation under Award 2212506.

## References

- [1] Kartik Ahuja, Divyat Mahajan, Yixin Wang, and Yoshua Bengio. Interventional causal representation learning. In *International Conference on Machine Learning*, pages 372–407. PMLR, 2023.
- [2] Jochen Arnhold, Peter Grassberger, Klaus Lehnertz, and Christian Erich Elger. A robust method for detecting interdependences: application to intracranially recorded EEG. *Physica D: Nonlinear Phenomena*, 134(4):419–430, 1999.

- [3] Zsigmond Benkő, Ádám Zlatniczki, Marcell Stipplinger, Dániel Fabó, András Sólyom, Loránd Erőss, András Telcs, and Zoltán Somogyvári. Bayesian inference of causal relations between dynamical systems. *Chaos, Solitons & Fractals*, 185:115142, 2024.
- [4] Patrick Blöbaum, Dominik Janzing, Takashi Washio, Shohei Shimizu, and Bernhard Schölkopf. Cause-effect inference by comparing regression errors. In *International Conference on Artificial Intelligence and Statistics*, pages 900–909. PMLR, 2018.
- [5] Leo Breston, Eric J Leonardis, Laleh K Quinn, Michael Tolston, Janet Wiles, and Andrea A Chiba. Convergent cross sorting for estimating dynamic coupling. *Scientific Reports*, 11(1):20374, 2021.
- [6] Kurt Butler, Guanchao Feng, and Petar M Djurić. On causal discovery with convergent cross mapping. *IEEE Transactions on Signal Processing*, 2023.
- [7] Adam Thomas Clark, Hao Ye, Forest Isbell, Ethan R Deyle, Jane Cowles, G David Tilman, and George Sugihara. Spatial convergent cross mapping to detect causal relationships from short time series. *Ecology*, 96(5):1174–1181, 2015.
- [8] Sarah Cobey and Edward B Baskerville. Limits to causal inference with state-space reconstruction for infectious disease. *PloS one*, 11(12):e0169050, 2016.
- [9] Thomas M. Cover and Joy A. Thomas. *Elements of Information Theory*. Wiley-Interscience, USA, 2006.
- [10] Paweł Czyż, Frederic Grabowski, Julia E Vogt, Niko Beerewinkel, and Alexander Marx. Beyond normal: On the evaluation of mutual information estimators. In *Thirty-seventh Conference on Neural Information Processing Systems*, 2023.
- [11] Povilas Daniušis, Dominik Janzing, Joris Mooij, Jakob Zscheischler, Bastian Steudel, Kun Zhang, and Bernhard Schölkopf. Inferring deterministic causal relations. In *Proceedings of the Twenty-Sixth Conference on Uncertainty in Artificial Intelligence*, pages 143–150, 2010.
- [12] Edward De Brouwer, Adam Arany, Jaak Simm, and Yves Moreau. Latent convergent cross mapping. In *International Conference on Learning Representations*, 2020.
- [13] Guanchao Feng, Kezi Yu, Yunlong Wang, Yilian Yuan, and Petar M Djurić. Improving convergent cross mapping for causal discovery with Gaussian processes. In *2020 IEEE International Conference on Acoustics, Speech and Signal Processing (ICASSP)*, pages 3692–3696. IEEE, 2020.
- [14] Bingbo Gao, Jianyu Yang, Ziyue Chen, George Sugihara, Manchun Li, Alfred Stein, Mei-Po Kwan, and Jinfeng Wang. Causal inference from cross-sectional earth system data with geographical convergent cross mapping. *Nature Communications*, 14(1):5875, 2023.
- [15] Clive WJ Granger. Investigating causal relations by econometric models and cross-spectral methods. *Econometrica: Journal of the Econometric Society*, pages 424–438, 1969.
- [16] Michael T Heath. *Scientific Computing: An Introductory Survey*. SIAM, 2018.
- [17] Patrik Hoyer, Dominik Janzing, Joris M Mooij, Jonas Peters, and Bernhard Schölkopf. Nonlinear causal discovery with additive noise models. *Advances in Neural Information Processing Systems*, 21, 2008.
- [18] Diviyan Kalainathan, Olivier Goudet, and Ritik Dutta. Causal discovery toolbox: Uncovering causal relationships in Python. *Journal of Machine Learning Research*, 21(37):1–5, 2020.
- [19] Matthew B Kennel, Reggie Brown, and Henry DI Abarbanel. Determining embedding dimension for phase-space reconstruction using a geometrical construction. *Physical Review A*, 45(6):3403, 1992.
- [20] Alexander Kraskov, Harald Stögbauer, and Peter Grassberger. Estimating mutual information. *Physical Review E*, 69(6):066138, 2004.

[21] Dimitris Kugiumtzis. State space reconstruction parameters in the analysis of chaotic time series—the role of the time window length. *Physica D: Nonlinear Phenomena*, 95(1):13–28, 1996.

[22] John M Lee. *Introduction to Smooth Manifolds*, volume 218 of *Graduate Texts in Mathematics*. Springer, second edition, 2012.

[23] Huanfei Ma, Kazuyuki Aihara, and Luonan Chen. Detecting causality from nonlinear dynamics with short-term time series. *Scientific Reports*, 4(1):7464, 2014.

[24] A. McInerney. *First Steps in Differential Geometry: Riemannian, Contact, Symplectic*. Undergraduate Texts in Mathematics. Springer New York, 2013.

[25] Dan Mønster, Riccardo Fusaroli, Kristian Tylén, Andreas Roepstorff, and Jacob F Sherson. Causal inference from noisy time-series data—testing the convergent cross-mapping algorithm in the presence of noise and external influence. *Future Generation Computer Systems*, 73:52–62, 2017.

[26] Francesco Orabona and Tatiana Tommasi. Training deep networks without learning rates through coin betting. *Advances in Neural Information Processing Systems*, 30, 2017.

[27] Judea Pearl. *Causality*. Cambridge University Press, 2009.

[28] R Quian Quiroga, Jochen Arnhold, and Peter Grassberger. Learning driver-response relationships from synchronization patterns. *Physical Review E*, 61(5):5142, 2000.

[29] Nikolai F Rulkov, Mikhail M Sushchik, Lev S Tsimring, and Henry DI Abarbanel. Generalized synchronization of chaos in directionally coupled chaotic systems. *Physical Review E*, 51(2):980, 1995.

[30] Jakob Runge, Andreas Gerhardus, Gherardo Varando, Veronika Eyring, and Gustau Camps-Valls. Causal inference for time series. *Nature Reviews Earth & Environment*, 4(7):487–505, 2023.

[31] Jakob Runge, Vladimir Petoukhov, Jonathan F Donges, Jaroslav Hlinka, Nikola Jajcay, Martin Vejmelka, David Hartman, Norbert Marwan, Milan Paluš, and Jürgen Kurths. Identifying causal gateways and mediators in complex spatio-temporal systems. *Nature Communications*, 6(1):8502, 2015.

[32] Tim Sauer. Reconstruction of dynamical systems from interspike intervals. *Physical Review Letters*, 72(24):3811, 1994.

[33] Tim Sauer, James A Yorke, and Martin Casdagli. Embedology. *Journal of Statistical Physics*, 65:579–616, 1991.

[34] Abraham Savitzky and Marcel JE Golay. Smoothing and differentiation of data by simplified least squares procedures. *Analytical Chemistry*, 36(8):1627–1639, 1964.

[35] Steven J Schiff, Paul So, Taeun Chang, Robert E Burke, and Tim Sauer. Detecting dynamical interdependence and generalized synchrony through mutual prediction in a neural ensemble. *Physical Review E*, 54(6):6708, 1996.

[36] Bernhard Schölkopf, Francesco Locatello, Stefan Bauer, Nan Rosemary Ke, Nal Kalchbrenner, Anirudh Goyal, and Yoshua Bengio. Toward causal representation learning. *Proceedings of the IEEE*, 109(5):612–634, 2021.

[37] Skipper Seabold and Josef Perktold. statsmodels: Econometric and statistical modeling with Python. In *9th Python in Science Conference*, 2010.

[38] Ercan Solak, Roderick Murray-Smith, WE Leithead, Douglas Leith, and Carl Rasmussen. Derivative observations in Gaussian process models of dynamic systems. *Advances in Neural Information Processing Systems*, 15, 2002.

[39] Jaroslav Stark. Delay embeddings for forced systems. I. Deterministic forcing. *Journal of Nonlinear Science*, 9:255–332, 1999.

- [40] Jaroslav Stark, David S Broomhead, Michael Evan Davies, and J Huke. Delay embeddings for forced systems. II. Stochastic forcing. *Journal of Nonlinear Science*, 13:519–577, 2003.
- [41] George Sugihara, Robert May, Hao Ye, Chih-hao Hsieh, Ethan Deyle, Michael Fogarty, and Stephan Munch. Detecting causality in complex ecosystems. *Science*, 338(6106):496–500, 2012.
- [42] Floris Takens. Detecting strange attractors in turbulence. In David Rand and Lai-Sang Young, editors, *Dynamical Systems and Turbulence, Warwick 1980*, pages 366–381, Berlin, Heidelberg, 1981. Springer.
- [43] Gherardo Varando, Miguel-Ángel Fernández-Torres, Jordi Muñoz-Marí, and Gustau Camps-Valls. Learning causal representations with Granger PCA. In *UAI 2022 Workshop on Causal Representation Learning*, 2022.
- [44] Hao Ye, Ethan R Deyle, Luis J Gilarranz, and George Sugihara. Distinguishing time-delayed causal interactions using convergent cross mapping. *Scientific Reports*, 5(1):14750, 2015.
- [45] Hao Ye and George Sugihara. Information leverage in interconnected ecosystems: Overcoming the curse of dimensionality. *Science*, 353(6302):922–925, 2016.
- [46] Yujia Zheng, Biwei Huang, Wei Chen, Joseph Ramsey, Mingming Gong, Ruichu Cai, Shohei Shimizu, Peter Spirtes, and Kun Zhang. Causal-learn: Causal discovery in Python. *Journal of Machine Learning Research*, 25(60):1–8, 2024.

## A Important Facts About Manifolds

In this appendix, we review some important background about manifolds. Much more complete references include the authoritative [22] (especially chapters 1, 2, 3, and 8), or the more accessible [24].

We say that a function  $F$  is *smooth* if it has derivatives of all orders. A *diffeomorphism* is a function  $F$  which is smooth, invertible, and  $F^{-1}$  is also smooth. We say that two subsets  $M$  and  $N$  of  $\mathbb{R}^n$  are diffeomorphic if there exists a *diffeomorphism* such that  $F(M) = N$ .

A subset  $M$  of  $\mathbb{R}^n$  is called a  **$d$ -dimensional manifold** if for every point  $x$  in  $M$ , there exists an open set  $U_x$  such that

1. There is a diffeomorphism  $F_x : \mathbb{R}^n \rightarrow U_x$ .
2. The image of the set  $\mathbb{H}_d = \{y \in \mathbb{R}^n : y_{d+1} = \dots = y_n = 0\}$  under  $F_x$  is given by

$$F_x(\mathbb{H}_d) = U_x \cap M.$$

Without a loss of generality, we can assume that  $F_x(0) = x$  in this definition. This allows us to easily define tangent vectors. A vector  $v \in \mathbb{R}^n$  is called a **tangent vector** of  $M$  at the point  $x$  if there exists a path  $\gamma(t)$  in  $\mathbb{H}_d$  such that

$$\frac{d}{dt} (F_x(\gamma(t)))|_{t=0} = v,$$

where  $F_x$  is the diffeomorphism in the above definition. The **tangent space**  $T_x M$  is defined to be the set of all tangent vectors of  $M$  at  $x$ . Note that from these definitions, it is clear that  $\mathbb{R}^n$  is a manifold and  $T_x \mathbb{R}^d = \mathbb{R}^d$ .

In calculus, we define a vector field  $\mathbf{u}$  on  $\mathbb{R}^n$  to be a function  $\mathbf{u} : \mathbb{R}^n \rightarrow \mathbb{R}^n$ . We generalize this to manifolds in Euclidean space by defining a **vector field  $\mathbf{u}$  on  $M$**  to be a mapping  $\mathbf{u} : M \rightarrow \mathbb{R}^n$  such that  $\mathbf{u}(x) \in T_x M$  at every point  $x$ .

An *embedding* of a manifold  $M \subset \mathbb{R}^n$  is a mapping  $F : \mathbb{R}^n \rightarrow \mathbb{R}^m$  such that  $F$  restricted to  $M$  is a diffeomorphism onto its image. If  $M$  is a manifold of dimension  $d$  and  $F$  is an embedding, then  $m$  is necessarily greater than or equal to  $d$ . In general, it is an interesting question to ask how much larger  $m$  must be so that embeddings are easy to find. The Whitney embedding theorem says that it is a generic property that  $F : \mathbb{R}^n \rightarrow \mathbb{R}^m$  when  $m \geq 2d + 1$ . Takens' theorem refines the Whitney theorem by asserting that such an embedding can be obtained from a scalar observation function, by time lagging the observations sufficiently many times.

## B Additional Experiments

In this appendix, we include experiments and results omitted from the main text.

### B.1 Varying Embedding Dimension

One of the key parameters in both CCM and TSCI is the embedding dimension parameter  $Q$  used during reconstruction of the shadow manifold. Takens' theorem suggests that once  $Q$  reaches a certain value, the manifold is embedded and the improvement of the results should saturate in principle. Of course, in real life there is a curse of dimensionality associated with inference, so it is interesting to check how well the results behave as the embedding dimension is chosen to be higher than necessary. We consider the effect of varying the parameter  $Q$  using data from the Rössler-Lorenz system in Fig. 4. Performance of both methods improve as the dimension of the putative effect (if we are testing  $x \rightarrow y$ , then this is  $Q_y$ ) is increased, until saturating after the manifolds are fully embedded.

### B.2 Corrupted Signals

Generally, there are many non-trivial ways in which the state reconstruction can be poor, e.g., presence of periodic trends [8] and underexploration of the shadow manifold [6]. We consider two scenarios that deteriorate the state reconstruction quality on the Rössler-Lorenz system: additive noise, and a periodic trend.

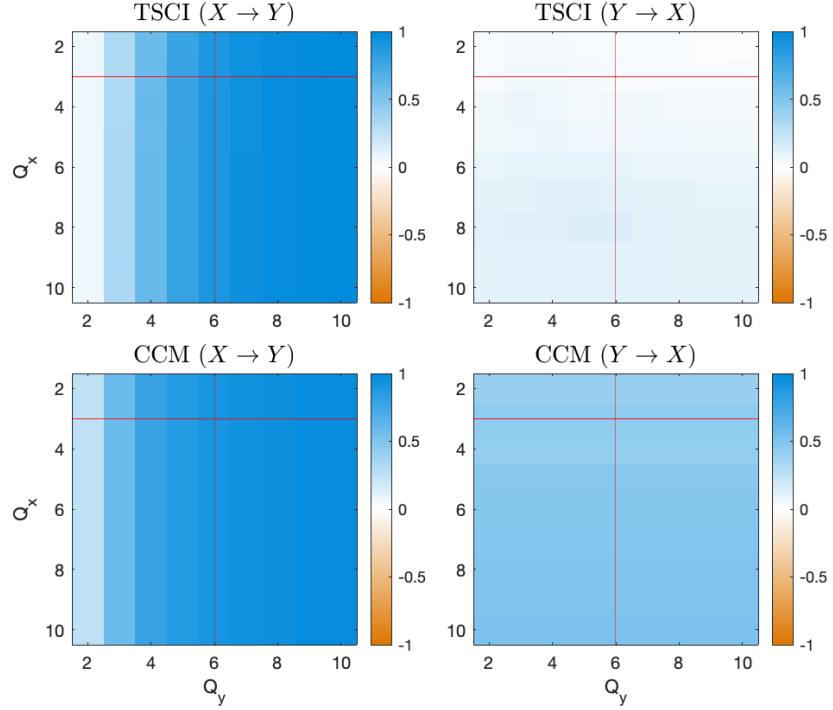


Figure 4: Comparison of TSCI and CCM for the unidirectionally coupled Rössler-Lorenz system Eq. (13) with  $C = 1$ . Here,  $x(t) = z_2(t)$  and  $y(t) = z_4(t)$ , and the true causality is  $x \rightarrow y$ . The red lines indicate the values of  $Q_x$  and  $Q_y$  selected by false-nearest neighbors with a tolerance of 0.01.

Results for additive noise are presented in Fig. 5. We fixed  $C = 1.0$  and varied the signal-to-noise ratio (SNR) from 0 dB to 60 dB by adding Gaussian noise to the observed signals. When estimating derivatives, a Savitzky-Golay filter [34] was used with a window length of 5 and order 2.

Overall, we find the performance relative to SNR to be similar between CCM and TSCI, suggesting that inference of the vector field from noisy data is not a limiting factor in the presence of additive noise.

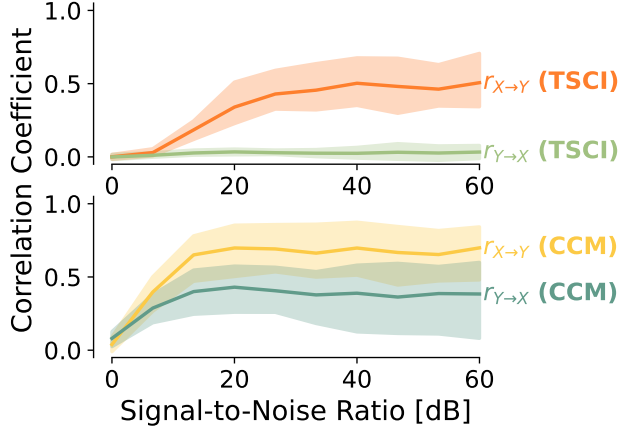


Figure 5: Comparison of TSCI with CCM for the Rössler-Lorenz system (true causation  $X \rightarrow Y$ ) with additive noise. The plotted lines show the median test statistic over 100 trials for both CCM and TSCI, and the shaded region indicates the 5th and 95th percentiles when (a)  $C$  is fixed to 1.0 and the signal-to-noise ratio is varied.

An alternative way to corrupt signals is with a deterministic periodic trend; we used a sine wave with a period of  $2\pi$ , and varied its power with respect to the true signal. Results are presented in Fig. 6. Our takeaways are relatively similar to the additive noise experiment: TSCI seems to degrade similarly to CCM, but its increased separation between cause and effect makes this degradation in performance less problematic. Notably, TSCI seems significantly more robust to false claims of strong causation when the relative power of the confounder is large.

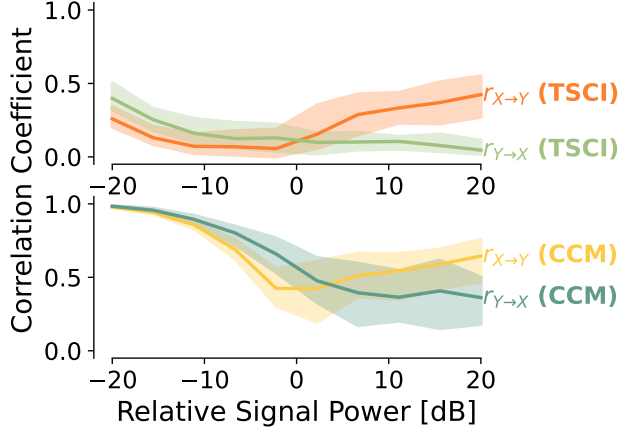


Figure 6: Results of the Rössler-Lorenz system with  $C = 1$  corrupted by an additive sine signal of varying amplitude. The amplitude of the signal, relative to the sine wave, is plotted in decibels on the horizontal axis.

### B.3 Using the Mutual Information for Scores

One interesting alternative to the cosine similarity score is the mutual information (MI), which provides a non-linear quantification of how related  $\mathbf{u}$  and  $\mathbf{J}_F \mathbf{v}$  are. One immediate concern with using MI is that estimates from finite samples are difficult; we use the classical estimator of Kraskov, Stögbauer, and Grassberger [20], which has shown relevance even in the era of deep learning [10].

Results on the Rössler-Lorenz test system while varying the coupling parameter  $C$  are presented in Fig. 7. We find that MI typically shows less separation than TSCI, which brings into question its viability when the ground truth is unknown. Another issue is in the interpretation of MI estimates: it is not entirely clear if an MI estimate of, for example, 1 nat indicates strong influence, and MI estimates are not easily normalized in the continuous setting.

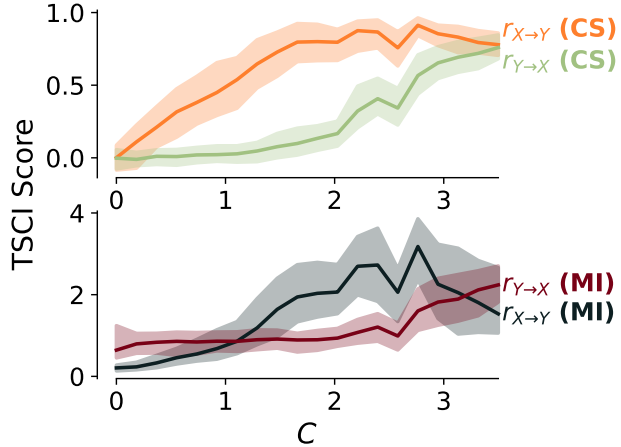


Figure 7: Results of the Rössler-Lorenz system using the cosine similarity and mutual information while varying  $C$ . Compare to Figure 2a in the main manuscript.

#### B.4 Comparisons to Other Causal Discovery Methods

As argued in the main manuscript, cross-map-based methods such as TSCI and CCM approach causal discovery in a rather particular setting, where more mainstream methods do not apply. We empirically verify these claims on the Rössler-Lorenz test system, using a variety of values of  $C$ . We compare against Granger causality, as well as various bivariate causal discovery methods.

We first compare against Granger causality in Table 2. As expected from the theory, Granger causality incorrectly infers bidirectional causality for all  $C > 0$ .

We also compare against various methods from the bivariate or pairwise causal discovery literature. These methods typically assume the existence of a map  $y = f(x)$  which is either deterministic or subject to additive noise, which does not exist in all but the most trivial dynamical systems. This includes RECI [4], IGCI [11], and ANM [17]. Results are presented in Tables 3 and 4.

We find that IGCI consistently fails to detect a causal edge, with weak coefficients. RECI consistently chooses the direction  $X \rightarrow Y$ , but does so even when  $C = 0$ , which suggests that results are not actually detecting causality, but rather some other anomaly of the data. To this end, the variance ratios as described by Blobaum et al. [4] are typically large, indicating little confidence. Finally, for all  $C > 0$ , ANM detects bidirectional causality.

Comparisons with Granger causality use the implementation of `statsmodels`<sup>8</sup> [37]. All comparisons to RECI and IGCI used the implementations of `cdt`<sup>9</sup> [18], with a minor bug-fix for RECI. Comparisons with ANM used the implementation of `causal-learn`<sup>10</sup> [46].

Table 2: Granger Causal Results for Rössler-Lorenz System. Entries denote the median, 5th, and 95th percentile p-values across 50 trials. All p-values are from the F-test implemented in `statstools`.

| $C$  | p-value $X \rightarrow Y$               | p-value $Y \rightarrow X$               |
|------|---|---|
| 0.0  | 0.003 <sub>0.000</sub> <sup>0.345</sup> | 0.168 <sub>0.000</sub> <sup>0.896</sup> |
| 0.75 | 0.000 <sub>0.000</sub> <sup>0.000</sup> | 0.000 <sub>0.000</sub> <sup>0.000</sup> |
| 1.5  | 0.000 <sub>0.000</sub> <sup>0.000</sup> | 0.000 <sub>0.000</sub> <sup>0.000</sup> |
| 2.25 | 0.000 <sub>0.000</sub> <sup>0.000</sup> | 0.000 <sub>0.000</sub> <sup>0.000</sup> |
| 3.0  | 0.000 <sub>0.000</sub> <sup>0.000</sup> | 0.000 <sub>0.000</sub> <sup>0.000</sup> |

Table 3: Bivariate causal discovery results for Rössler-Lorenz System. For all models, a negative score indicates  $X \rightarrow Y$  and a positive score indicates  $Y \rightarrow X$ . All scores are based on the implementations of `cdt`. Entries denote the median, min, and max over 10 trials.

| $C$  | RECI                                       | IGCI                                      |
|------|--|---|
| 0.0  | -0.021 <sub>-0.027</sub> <sup>-0.017</sup> | 0.035 <sub>0.018</sub> <sup>0.074</sup>   |
| 0.75 | -0.025 <sub>-0.048</sub> <sup>-0.019</sup> | 0.034 <sub>-0.017</sub> <sup>0.048</sup>  |
| 1.5  | -0.028 <sub>-0.039</sub> <sup>-0.025</sup> | -0.016 <sub>-0.078</sub> <sup>0.031</sup> |
| 2.25 | -0.029 <sub>-0.036</sub> <sup>-0.027</sup> | 0.040 <sub>0.004</sub> <sup>0.073</sup>   |
| 3.0  | -0.036 <sub>-0.041</sub> <sup>-0.017</sup> | 0.030 <sub>0.011</sub> <sup>0.042</sup>   |

## C Proofs

In this section, we provide proofs for results mentioned in the main text.

**Proof of Theorem 2.1** There are many different proofs and versions of Takens' theorem. This version is proved by Sauer, Yorke and Casdagli [33], and is beyond the scope of this appendix. Other noteworthy variations of this theorem are proved by Stark [39] and Stark et al. [40].  $\square$

<sup>8</sup><https://github.com/statsmodels/statsmodels/>, BSD-3-Clause License

<sup>9</sup><https://github.com/FenTechSolutions/CausalDiscoveryToolbox>, MIT License

<sup>10</sup><https://github.com/py-why/causal-learn>, MIT License

Table 4: ANM causal discovery results for Rössler-Lorenz System. Entries denote the median, min, and max  $p$ -value over 10 trials. All scores are based on the implementation in `causal-learn`.

| $C$  | $X \rightarrow Y$       | $Y \rightarrow X$       |
|------|-------------------------|-------------------------|
| 0.0  | $0.507^{0.777}_{0.096}$ | $0.450^{0.915}_{0.003}$ |
| 0.75 | $0.000^{0.121}_{0.000}$ | $0.000^{0.049}_{0.000}$ |
| 1.5  | $0.000^{0.000}_{0.000}$ | $0.000^{0.000}_{0.000}$ |
| 2.25 | $0.000^{0.000}_{0.000}$ | $0.000^{0.000}_{0.000}$ |
| 3.0  | $0.000^{0.000}_{0.000}$ | $0.000^{0.000}_{0.000}$ |

**Proof of Corollary 2.1.1** Let us assume that we have a generic system, where  $(\mathbf{z}_x, \mathbf{z}_y) \in M$  for some manifold  $M$ , and  $x$  is a function  $\mathbf{z}_x$  and  $y$  is a function of  $\mathbf{z}_y$ .

If  $x \rightarrow y$  and  $x \leftarrow y$  both hold, then  $\mathcal{M}_x$  and  $\mathcal{M}_y$  are both diffeomorphic to  $M$ , and thus, diffeomorphic to each other. The existence of a cross map is then immediate.

If  $x \rightarrow y$  but not vice-versa, then the dynamics of  $\mathbf{z}_x$  are autonomous, meaning that the behavior of  $\mathbf{z}_x$  depends only upon itself. As a result, the projection map  $\pi_x(\mathbf{z}_x, \mathbf{z}_y) = \mathbf{z}_x$  can be applied directly to  $M$  to yield a new manifold  $M_x$  on which  $\mathbf{z}_x$  is an autonomous dynamical system. Since  $x$  observes this system  $\mathbf{z}_x$ ,  $\mathcal{M}_x$  will be diffeomorphic to  $M_x$ , since  $\mathbf{z}_x$  only contains information about  $\mathbf{z}_x$ . Let  $\Phi_x : M_x \rightarrow \mathcal{M}_x$  and  $\Phi_y : M \rightarrow \mathcal{M}_y$  denote the diffeomorphisms implied by Takens' theorem. We can construct the cross map then as

$$F(\tilde{\mathbf{y}}) = \Phi_x(\pi_x(\Phi_y^{-1}(\tilde{\mathbf{y}}))).$$

□

**Proof of Corollary 2.1.2** Since the shadow manifold  $\mathcal{M}$  produced by Takens' theorem is a smooth embedding of the original manifold  $M$ , there exists a diffeomorphism  $\Phi : M \rightarrow \mathcal{M}$ . By Proposition 8.19 of Lee [22, p. 183], for any given vector field  $\mathbf{u}$  defined on  $M$ , there exists a unique vector field  $\mathbf{v}$  on  $\mathcal{M}$  that is the push forward of  $\mathbf{u}$  under the map  $\Phi$ . Because the dynamics on the manifold are derived from these vector fields, the two systems are equivalent as dynamical systems. □

**Proof of Lemma 2.1.1** Suppose that  $F : \mathcal{M}_x \rightarrow \mathcal{M}_y$  is a cross map. Fix any point  $\tilde{\mathbf{x}}_0 \in \mathcal{M}_x$  and let  $\tilde{\mathbf{y}}_0 = F(\tilde{\mathbf{x}}_0)$ . If we consider flows forwards and backwards with respect to these vector fields, then there exists some small  $\varepsilon > 0$  such that we have curves  $\tilde{\mathbf{x}}_t$  along  $\mathcal{M}_x$  and  $\tilde{\mathbf{y}}_t$  along  $\mathcal{M}_y$  such that  $\tilde{\mathbf{y}}_t = F(\tilde{\mathbf{x}}_t)$  for each  $t$  in the interval  $(-\varepsilon, \varepsilon)$ . By the chain rule of calculus, we have that

$$\frac{d\tilde{\mathbf{y}}_0}{dt} = \mathbf{J}_F(\tilde{\mathbf{x}}_0) \frac{d\tilde{\mathbf{x}}_0}{dt},$$

where  $\mathbf{J}_F(\tilde{\mathbf{x}})$  is the Jacobian matrix of the function  $F$  at the point  $\tilde{\mathbf{x}}$ . Since the dynamics of these spaces are given by vector fields, we can replace the time derivatives in the equation with their vector fields:

$$\mathbf{v}(\tilde{\mathbf{y}}_0) = \mathbf{J}_F(\tilde{\mathbf{x}}_0) \mathbf{u}(\tilde{\mathbf{x}}_0).$$

Since the point  $\tilde{\mathbf{x}}_0$  that we chose was arbitrary, the statement holds for every point in  $\mathcal{M}_x$ . □

## NeurIPS Paper Checklist

### 1. Claims

Question: Do the main claims made in the abstract and introduction accurately reflect the paper's contributions and scope?

Answer: [\[Yes\]](#)

Justification: The abstract and introduction have been written to clearly state our claims and contributions of the paper.

Guidelines:

- The answer NA means that the abstract and introduction do not include the claims made in the paper.
- The abstract and/or introduction should clearly state the claims made, including the contributions made in the paper and important assumptions and limitations. A No or NA answer to this question will not be perceived well by the reviewers.
- The claims made should match theoretical and experimental results, and reflect how much the results can be expected to generalize to other settings.
- It is fine to include aspirational goals as motivation as long as it is clear that these goals are not attained by the paper.

### 2. Limitations

Question: Does the paper discuss the limitations of the work performed by the authors?

Answer: [\[Yes\]](#)

Justification: The paper discusses the limitations and assumptions of the approach, and the possible failure modes. A section discussing the advantages and limitations of the approach has also been included in the paper.

Guidelines:

- The answer NA means that the paper has no limitation while the answer No means that the paper has limitations, but those are not discussed in the paper.
- The authors are encouraged to create a separate "Limitations" section in their paper.
- The paper should point out any strong assumptions and how robust the results are to violations of these assumptions (e.g., independence assumptions, noiseless settings, model well-specification, asymptotic approximations only holding locally). The authors should reflect on how these assumptions might be violated in practice and what the implications would be.
- The authors should reflect on the scope of the claims made, e.g., if the approach was only tested on a few datasets or with a few runs. In general, empirical results often depend on implicit assumptions, which should be articulated.
- The authors should reflect on the factors that influence the performance of the approach. For example, a facial recognition algorithm may perform poorly when image resolution is low or images are taken in low lighting. Or a speech-to-text system might not be used reliably to provide closed captions for online lectures because it fails to handle technical jargon.
- The authors should discuss the computational efficiency of the proposed algorithms and how they scale with dataset size.
- If applicable, the authors should discuss possible limitations of their approach to address problems of privacy and fairness.
- While the authors might fear that complete honesty about limitations might be used by reviewers as grounds for rejection, a worse outcome might be that reviewers discover limitations that aren't acknowledged in the paper. The authors should use their best judgment and recognize that individual actions in favor of transparency play an important role in developing norms that preserve the integrity of the community. Reviewers will be specifically instructed to not penalize honesty concerning limitations.

### 3. Theory Assumptions and Proofs

Question: For each theoretical result, does the paper provide the full set of assumptions and a complete (and correct) proof?

Answer: [\[Yes\]](#)

Justification: We have taken care to provide precise mathematical statements and proofs. For proofs which we do not provide (like the proof of Takens' theorem), we reference other sources where the proof may be found.

Guidelines:

- The answer NA means that the paper does not include theoretical results.
- All the theorems, formulas, and proofs in the paper should be numbered and cross-referenced.
- All assumptions should be clearly stated or referenced in the statement of any theorems.
- The proofs can either appear in the main paper or the supplemental material, but if they appear in the supplemental material, the authors are encouraged to provide a short proof sketch to provide intuition.
- Inversely, any informal proof provided in the core of the paper should be complemented by formal proofs provided in appendix or supplemental material.
- Theorems and Lemmas that the proof relies upon should be properly referenced.

#### 4. Experimental Result Reproducibility

Question: Does the paper fully disclose all the information needed to reproduce the main experimental results of the paper to the extent that it affects the main claims and/or conclusions of the paper (regardless of whether the code and data are provided or not)?

Answer: [\[Yes\]](#)

Justification: We have worked to make our results as reproducible as possible. We have provided a full description of the TSCI algorithm so that a reader should be able to implement and reproduce our method from the written manuscript. The design of the experiments has also be described within reason, so that any factor that might determine their outcome has been detailed. For minor technical details (such as the type of ODE solver used to generate data) which are less likely affect the results of the experiment, we refer to the code included with the paper.

Guidelines:

- The answer NA means that the paper does not include experiments.
- If the paper includes experiments, a No answer to this question will not be perceived well by the reviewers: Making the paper reproducible is important, regardless of whether the code and data are provided or not.
- If the contribution is a dataset and/or model, the authors should describe the steps taken to make their results reproducible or verifiable.
- Depending on the contribution, reproducibility can be accomplished in various ways. For example, if the contribution is a novel architecture, describing the architecture fully might suffice, or if the contribution is a specific model and empirical evaluation, it may be necessary to either make it possible for others to replicate the model with the same dataset, or provide access to the model. In general, releasing code and data is often one good way to accomplish this, but reproducibility can also be provided via detailed instructions for how to replicate the results, access to a hosted model (e.g., in the case of a large language model), releasing of a model checkpoint, or other means that are appropriate to the research performed.
- While NeurIPS does not require releasing code, the conference does require all submissions to provide some reasonable avenue for reproducibility, which may depend on the nature of the contribution. For example
  - (a) If the contribution is primarily a new algorithm, the paper should make it clear how to reproduce that algorithm.
  - (b) If the contribution is primarily a new model architecture, the paper should describe the architecture clearly and fully.
  - (c) If the contribution is a new model (e.g., a large language model), then there should either be a way to access this model for reproducing the results or a way to reproduce the model (e.g., with an open-source dataset or instructions for how to construct the dataset).

(d) We recognize that reproducibility may be tricky in some cases, in which case authors are welcome to describe the particular way they provide for reproducibility. In the case of closed-source models, it may be that access to the model is limited in some way (e.g., to registered users), but it should be possible for other researchers to have some path to reproducing or verifying the results.

## 5. Open access to data and code

Question: Does the paper provide open access to the data and code, with sufficient instructions to faithfully reproduce the main experimental results, as described in supplemental material?

Answer: [\[Yes\]](#)

Justification: Code to reproduce our results is being included with the publication, with MIT license. The code is reasonably organized and documented, and instructions on how to use the code have been included with the code itself. When making use of other code bases for comparison (e.g., with latent CCM), a link to the original code base was provided.

Guidelines:

- The answer NA means that paper does not include experiments requiring code.
- Please see the NeurIPS code and data submission guidelines (<https://nips.cc/public/guides/CodeSubmissionPolicy>) for more details.
- While we encourage the release of code and data, we understand that this might not be possible, so “No” is an acceptable answer. Papers cannot be rejected simply for not including code, unless this is central to the contribution (e.g., for a new open-source benchmark).
- The instructions should contain the exact command and environment needed to run to reproduce the results. See the NeurIPS code and data submission guidelines (<https://nips.cc/public/guides/CodeSubmissionPolicy>) for more details.
- The authors should provide instructions on data access and preparation, including how to access the raw data, preprocessed data, intermediate data, and generated data, etc.
- The authors should provide scripts to reproduce all experimental results for the new proposed method and baselines. If only a subset of experiments are reproducible, they should state which ones are omitted from the script and why.
- At submission time, to preserve anonymity, the authors should release anonymized versions (if applicable).
- Providing as much information as possible in supplemental material (appended to the paper) is recommended, but including URLs to data and code is permitted.

## 6. Experimental Setting/Details

Question: Does the paper specify all the training and test details (e.g., data splits, hyper-parameters, how they were chosen, type of optimizer, etc.) necessary to understand the results?

Answer: [\[Yes\]](#)

Justification: We have included all necessary details to understand and interpret the setup and results of the experimental section. Code is provided for the Rössler-Lorenz systems, and details on all networks, optimizers, and training details were provided for latent TSCI.

Guidelines:

- The answer NA means that the paper does not include experiments.
- The experimental setting should be presented in the core of the paper to a level of detail that is necessary to appreciate the results and make sense of them.
- The full details can be provided either with the code, in appendix, or as supplemental material.

## 7. Experiment Statistical Significance

Question: Does the paper report error bars suitably and correctly defined or other appropriate information about the statistical significance of the experiments?

Answer: [\[Yes\]](#)

Justification: In our experiments, we have provided suitable measures of the statistical confidence of our methods. In particular, we run over several folds and report either median/percentiles or mean/standard deviations of all results.

Guidelines:

- The answer NA means that the paper does not include experiments.
- The authors should answer "Yes" if the results are accompanied by error bars, confidence intervals, or statistical significance tests, at least for the experiments that support the main claims of the paper.
- The factors of variability that the error bars are capturing should be clearly stated (for example, train/test split, initialization, random drawing of some parameter, or overall run with given experimental conditions).
- The method for calculating the error bars should be explained (closed form formula, call to a library function, bootstrap, etc.)
- The assumptions made should be given (e.g., Normally distributed errors).
- It should be clear whether the error bar is the standard deviation or the standard error of the mean.
- It is OK to report 1-sigma error bars, but one should state it. The authors should preferably report a 2-sigma error bar than state that they have a 96% CI, if the hypothesis of Normality of errors is not verified.
- For asymmetric distributions, the authors should be careful not to show in tables or figures symmetric error bars that would yield results that are out of range (e.g. negative error rates).
- If error bars are reported in tables or plots, The authors should explain in the text how they were calculated and reference the corresponding figures or tables in the text.

## 8. Experiments Compute Resources

Question: For each experiment, does the paper provide sufficient information on the computer resources (type of compute workers, memory, time of execution) needed to reproduce the experiments?

Answer: [\[Yes\]](#)

Justification: We state in the experiments section that all code was run on a 6-Core Intel Core i5 CPU and NVIDIA Titan RTX GPU.

Guidelines:

- The answer NA means that the paper does not include experiments.
- The paper should indicate the type of compute workers CPU or GPU, internal cluster, or cloud provider, including relevant memory and storage.
- The paper should provide the amount of compute required for each of the individual experimental runs as well as estimate the total compute.
- The paper should disclose whether the full research project required more compute than the experiments reported in the paper (e.g., preliminary or failed experiments that didn't make it into the paper).

## 9. Code Of Ethics

Question: Does the research conducted in the paper conform, in every respect, with the NeurIPS Code of Ethics <https://neurips.cc/public/EthicsGuidelines>?

Answer: [\[Yes\]](#)

Justification: The research conducted in this paper is in compliance with the NeurIPS Code of Ethics.

Guidelines:

- The answer NA means that the authors have not reviewed the NeurIPS Code of Ethics.
- If the authors answer No, they should explain the special circumstances that require a deviation from the Code of Ethics.
- The authors should make sure to preserve anonymity (e.g., if there is a special consideration due to laws or regulations in their jurisdiction).

## 10. Broader Impacts

Question: Does the paper discuss both potential positive societal impacts and negative societal impacts of the work performed?

Answer: [Yes]

Justification: The paper includes discussion of the potential broader impact of the work in the introduction.

Guidelines:

- The answer NA means that there is no societal impact of the work performed.
- If the authors answer NA or No, they should explain why their work has no societal impact or why the paper does not address societal impact.
- Examples of negative societal impacts include potential malicious or unintended uses (e.g., disinformation, generating fake profiles, surveillance), fairness considerations (e.g., deployment of technologies that could make decisions that unfairly impact specific groups), privacy considerations, and security considerations.
- The conference expects that many papers will be foundational research and not tied to particular applications, let alone deployments. However, if there is a direct path to any negative applications, the authors should point it out. For example, it is legitimate to point out that an improvement in the quality of generative models could be used to generate deepfakes for disinformation. On the other hand, it is not needed to point out that a generic algorithm for optimizing neural networks could enable people to train models that generate Deepfakes faster.
- The authors should consider possible harms that could arise when the technology is being used as intended and functioning correctly, harms that could arise when the technology is being used as intended but gives incorrect results, and harms following from (intentional or unintentional) misuse of the technology.
- If there are negative societal impacts, the authors could also discuss possible mitigation strategies (e.g., gated release of models, providing defenses in addition to attacks, mechanisms for monitoring misuse, mechanisms to monitor how a system learns from feedback over time, improving the efficiency and accessibility of ML).

## 11. Safeguards

Question: Does the paper describe safeguards that have been put in place for responsible release of data or models that have a high risk for misuse (e.g., pretrained language models, image generators, or scraped datasets)?

Answer: [NA]

Justification: The paper does not pose any such risks for misuse.

Guidelines:

- The answer NA means that the paper poses no such risks.
- Released models that have a high risk for misuse or dual-use should be released with necessary safeguards to allow for controlled use of the model, for example by requiring that users adhere to usage guidelines or restrictions to access the model or implementing safety filters.
- Datasets that have been scraped from the Internet could pose safety risks. The authors should describe how they avoided releasing unsafe images.
- We recognize that providing effective safeguards is challenging, and many papers do not require this, but we encourage authors to take this into account and make a best faith effort.

## 12. Licenses for existing assets

Question: Are the creators or original owners of assets (e.g., code, data, models), used in the paper, properly credited and are the license and terms of use explicitly mentioned and properly respected?

Answer: [Yes]

Justification: We have provided in-text mentions and citations for all assets or methods that we used in this work.

Guidelines:

- The answer NA means that the paper does not use existing assets.
- The authors should cite the original paper that produced the code package or dataset.
- The authors should state which version of the asset is used and, if possible, include a URL.
- The name of the license (e.g., CC-BY 4.0) should be included for each asset.
- For scraped data from a particular source (e.g., website), the copyright and terms of service of that source should be provided.
- If assets are released, the license, copyright information, and terms of use in the package should be provided. For popular datasets, [paperswithcode.com/datasets](https://paperswithcode.com/datasets) has curated licenses for some datasets. Their licensing guide can help determine the license of a dataset.
- For existing datasets that are re-packaged, both the original license and the license of the derived asset (if it has changed) should be provided.
- If this information is not available online, the authors are encouraged to reach out to the asset's creators.

### 13. New Assets

Question: Are new assets introduced in the paper well documented and is the documentation provided alongside the assets?

Answer: [Yes]

Justification: We have included code with the publication that we have taken to document, organize, and make understandable for the future reader. Our code publication includes a proper license (MIT License) as well as instructions for use.

Guidelines:

- The answer NA means that the paper does not release new assets.
- Researchers should communicate the details of the dataset/code/model as part of their submissions via structured templates. This includes details about training, license, limitations, etc.
- The paper should discuss whether and how consent was obtained from people whose asset is used.
- At submission time, remember to anonymize your assets (if applicable). You can either create an anonymized URL or include an anonymized zip file.

### 14. Crowdsourcing and Research with Human Subjects

Question: For crowdsourcing experiments and research with human subjects, does the paper include the full text of instructions given to participants and screenshots, if applicable, as well as details about compensation (if any)?

Answer: [NA]

Justification: The current paper does not involve crowdsourcing nor research with human subjects.

Guidelines:

- The answer NA means that the paper does not involve crowdsourcing nor research with human subjects.
- Including this information in the supplemental material is fine, but if the main contribution of the paper involves human subjects, then as much detail as possible should be included in the main paper.
- According to the NeurIPS Code of Ethics, workers involved in data collection, curation, or other labor should be paid at least the minimum wage in the country of the data collector.

### 15. Institutional Review Board (IRB) Approvals or Equivalent for Research with Human Subjects

Question: Does the paper describe potential risks incurred by study participants, whether such risks were disclosed to the subjects, and whether Institutional Review Board (IRB) approvals (or an equivalent approval/review based on the requirements of your country or institution) were obtained?

Answer: [NA]

Justification: The current paper does not require IRB approval as it does not contain research with human or animal subjects.

Guidelines:

- The answer NA means that the paper does not involve crowdsourcing nor research with human subjects.
- Depending on the country in which research is conducted, IRB approval (or equivalent) may be required for any human subjects research. If you obtained IRB approval, you should clearly state this in the paper.
- We recognize that the procedures for this may vary significantly between institutions and locations, and we expect authors to adhere to the NeurIPS Code of Ethics and the guidelines for their institution.
- For initial submissions, do not include any information that would break anonymity (if applicable), such as the institution conducting the review.